Proc. Nat. Acad. Sci. USA
Vol. 70, No. 12, Part I, pp. 3604–3608, December 1973

Structure of Hemoglobin S Fibers: Optical Determination of the Molecular Orientation in Sickled Erythrocytes

(anemia/linear dichroism/microspectrophotometry/deoxyhemoglobin A crystals)

JAMES HOFRICHTER, DAVID G. HENDRICKER*, AND WILLIAM A. EATON

Laboratory of Chemical Physics, National Institute of Arthritis, Metabolism and Digestive Diseases, National Institutes of Health, Bethesda, Maryland 20014

Communicated by Donald S. Fredrickson, July 30, 1973

ABSTRACT **Possible orientations of deoxyhemoglobin S molecules within sickle-cell fibers are delimited by polarized absorption measurements on single sickled cells and single crystals of deoxyhemoglobin A. The polarization ratio of cells provides a lower limit for that of an individual fiber and, coupled with the absorption properties of the deoxyhemoglobin molecule, restricts the orientation of the long molecular (x) axis to within 22° of the fiber axis. Adopting the stacked ring model of Finch *et al.* for the molecular positions and the additional constraint that at least one mutated ($\beta 6$) site is part of an intermolecular contact, our optical result requires that the true molecular dyad (y) axis pass through some part of an adjacent molecule in the same ring. This range of orientations for the y axis is approximately perpendicular to those described in existing models and places at least one $\beta 6$ residue in position to be part of a contact between molecules in the same ring.**

The deformation that accompanies the deoxygenation of erythrocytes from patients with sickle-cell anemia is believed to result from the aggregation of hemoglobin molecules into an ordered phase. Crystallinity is evident from the linear birefringence (1–6) and dichroism (7, 8), and from the fiber-type x-ray diffraction patterns (9) of sickled cells and gels of deoxyhemoglobin S. Electron-microscope studies (6, 8, 10–14) indicate that the ordered phase is composed of bundles of long straight fibers, aligned parallel to each other as in a nematic liquid crystal. Finch *et al.* (8) have proposed a model for the individual fibers (Fig. 1), which appears to be consistent with both the electron-microscope and x-ray diffraction results. In this model the fiber may be described as a microtubule constructed from stacked rings of six hemoglobin molecules, where each ring is rotated slightly relative to the one below it. The structure can alternatively be viewed as six intertwined helical filaments, each having about 48 hemoglobin molecules per turn. If this model for the molecular positions is correct, then a knowledge of the precise molecular orientation should define the role of the mutation sites [Glu A3(6)β→Val] in forming intermolecular contacts within the fiber.

Neither electron microscopy nor x-ray diffraction has provided any concrete information on the molecular orientation. The hemoglobin molecule is a slightly elongated spheroid of dimensions 65 × 55 × 50 Å (15). The lack of significant shape anisotropy permits considerable freedom in packing hemoglobin molecules into a fiber of dimensions compatible with those found by electron microscopy and x-ray diffraction. In contrast to the physical ellipsoid, the ellipsoid that describes the absorption of plane-polarized light by a hemoglobin molecule is highly anisotropic (Fig. 2). One of the dimensions of this ellipsoid (x) is considerably shorter than the other two, and it is possible to obtain its precise orientation within the fiber from polarized absorption measurements. Visual observations of linear birefringence (1–6) and dichroism (7, 8) show that the x axis is more nearly parallel to the fiber axis than to the equatorial plane. In this communication we quantitate this result by measuring polarized absorption spectra on single sickled cells and single crystals of deoxyhemoglobin A using a microspectrophotometer. Our polarization data rigidly restrict the possible orientations of the x axis within the fiber, thereby placing an important constraint on models for its detailed structure.

OPTICAL THEORY

We shall relate the orientation of the hemoglobin molecule within the fiber to the polarized absorption of a sickled cell containing perfectly parallel fibers. First, we derive the optical absorption ellipsoid of the hemoglobin molecule from the known properties of the heme chromophore. We then express the orientation of the hemoglobin molecule in terms of this ellipsoid and the measured polarization ratio of the cell. Aside from geometric considerations, both steps require only that the interaction between hemes be negligible (17, 19–21).

The absorption ellipsoid of the hemoglobin molecule is defined by three principal extinction coefficients (22). One of these must lie along the true 2-fold axis, y. Because of the pseudo D_2 (222) molecular symmetry (15), the directions of the other two principal extinction coefficients correspond almost exactly to the pseudo-2-fold axes, x and z. The complete absorption ellipsoid has not been measured at any wavelength for deoxyhemoglobin S or A. It can, however, be reliably calculated for the Soret band, since optical studies on single crystals of various heme proteins show that the heme chromophore behaves like a nearly perfect planar absorber for this electronic transition (Makinen and Eaton, unpublished work) (17–20). Thus, at Soret wavelengths we obtain the molecular extinction coefficients by summing the squared projections of the four porphyrin planes onto the pseudo-2-fold axes.

$$\epsilon_k = \frac{3}{2}\bar{\epsilon}\sum_{\text{hemes}}\sin^2\theta_k \qquad [1]$$

The angle between the normal to the porphyrin plane and the kth molecular axis is θ_k ($k = x,y,z$), and $\bar{\epsilon}$ is the solution extinction coefficient per heme. The sum runs over all four hemes.

* On sabbatical leave from Department of Chemistry, Ohio University, Athens, Ohio 45701.

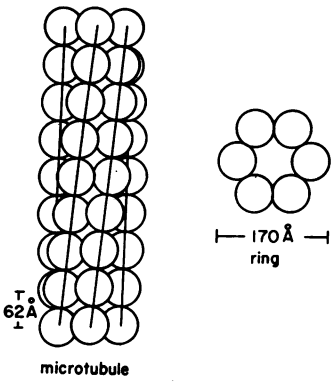

FIG. 1. Model of hemoglobin S fiber proposed by Finch *et al.* (8). Each circle represents a single hemoglobin molecule.

To calculate the fiber extinction coefficients, we assume that (*i*) either the fiber is uniaxial, or, if it is biaxial, that the sample under observation has uniaxial or random distribution about the fiber axis, and that (*ii*) all molecules have the same orientation with respect to the fiber axis. With these assumptions the extinction coefficients parallel and perpendicular to the fiber axis are given by:

$$\epsilon_{\parallel} = \sum_k \epsilon_k \cos^2 \phi_k \quad \text{and} \quad \epsilon_{\perp} = \frac{1}{2} \sum_k \epsilon_k \sin^2 \phi_k \qquad [2]$$

where ϕ_k is the angle between the kth molecular axis and the fiber axis. The measured quantity is the polarization ratio, P, and is defined by:

$$P \equiv \epsilon_{\perp}/\epsilon_{\parallel} = (\sum_k \epsilon_k \sin^2 \phi_k)/(2\sum_k \epsilon_k \cos^2 \phi_k) \qquad [3]$$

To proceed further we must consider the relative values of the ϵ_ks and anticipate the results that $\epsilon_x < \epsilon_y < \epsilon_z$ and $P > \epsilon_z/\epsilon_y$. We can now determine the maximum and minimum values for $|\phi_x|$ that are consistent with a given P. The maximum ϕ_x is obtained for z constrained to the equatorial plane, while the minimum ϕ_x occurs for y parallel to the equatorial plane. The relevant expressions follow directly from Eq. **3**:

$$\cos^2 \phi_x{}^{\max} = \frac{2P\epsilon_y - \epsilon_z - \epsilon_x}{(\epsilon_y - \epsilon_x)(2P + 1)},$$

$$\cos^2 \phi_x{}^{\min} = \frac{2P\epsilon_z - \epsilon_y - \epsilon_x}{(\epsilon_z - \epsilon_x)(2P + 1)} \qquad [4]$$

Notice that ϕ_x depends only on the measured polarization ratio of the cell and the *relative* values of the molecular extinction coefficients ϵ_x, ϵ_y, and ϵ_z.

EXPERIMENTAL

A thin layer of freshly drawn whole blood from a patient with sickle-cell disease was sealed between closely spaced glass coverslips using dental wax. The preparation was then set aside at either 25°C or 37°C. Within 24 hr deoxygenation and sickling was complete. Polarized absorption spectra on single sickled cells were measured at room temperature on a microspectrophotometer similar to the one described (23). The instrument consists of a 150 W Hanovia xenon arc lamp, tandem quartermeter Ebert grating monochromators (Jarrell Ash) with a Glan polarizing prism mounted at the exit slit, and a Leitz Ortholux polarizing microscope with photometric attachment. The light is detected by a RCA 1P28 photomultiplier tube and Keithley 414S picoammeter. An image of a Leitz rectangular field diaphragm made from adjustable crossed slits was focussed on the cell by a Zeiss 100X (0.8 NA) Ultrafluar Pol objective used as a condenser. The cell was further masked by a pinhole stop in the image plane of the objective, another Zeiss 100X (1.25 NA) Ultrafluar. Measuring areas as small as 1 μm^2 could be readily masked for transmission measurements. The absorbance was measured at each wavelength with light polarized parallel and perpendicular to the long axis of the cell. For the reference intensities a clear area immediately adjacent to the cell was used. In order to accurately reposition the cell, the translation into and out of the measuring beam was produced by rotating the slightly decentered microscope stage.

Crystals of human deoxyhemoglobin A were prepared (24). These crystals are monoclinic and belong to the space group $P2_1$ with two molecules per unit cell (24–26). They were prepared for spectral measurements by washing with a deoxygenated salt solution having the composition of the mother liquor, except that sodium dithionite was substituted for ferrous citrate. A drop of this suspension was sealed between glass coverslips under nitrogen. X-ray precession photography on a large crystal from this suspension gave unit cell parameters identical to those reported (25). Polarized absorption spectra were measured on the (010) face, which we identified by both the x-ray photographs and measurement of interaxial angles. For these absorption measurements a pair of 32X Zeiss Ultrafluar Pol objectives (0.4 NA) was used.

Solutions of human oxyhemoglobin A and S were prepared (24). After the final centrifugation step, the supernatant was diluted 1:10 with distilled water and sealed under nitrogen in an 100-μm pathlength cuvette. Spontaneous deoxygenation was complete in 24–48 hr (27). Absorption spectra were measured with a Cary 14 recording spectrophotometer.

RESULTS

The experimental parameters required to determine the orientation of the hemoglobin molecule within the fiber are stipulated in Eq. **4**. We must determine the relative magnitudes of ϵ_x, ϵ_y, and ϵ_z, the principal extinction coefficients of a deoxyhemoglobin molecule, and the value of P, the polarization ratio of a single fiber. We use the x-ray structure of deoxyhemoglobin A crystals to calculate the molecular extinction coefficients and confirm the reliability of these values from optical measurements on identical crystals. To obtain the polarization ratio of a single fiber, we measured the polarization ratios of a large number of sickled cells. The lack of perfect alignment of fibers within these cells demands that we accept the highest measured value as a lower limit for the true value of the polarization ratio of a single fiber.

The x-ray structure of deoxyhemoglobin A has been solved at high resolution by L. F. Ten Eyck and A. Arnone, Cambridge University. Using the orientation of the porphyrin planes from the 2.5-Å electron-density map, kindly supplied to us by Dr. A. D. McLachlan, we have calculated the molecular absorption ellipsoid of deoxyhemoglobin A using Eq. **1**. The extinction coefficients in the x,y,z pseudo-2-fold axis system are:

$$\epsilon_x = {}^3/_2\,\bar{\epsilon}\ (0.88),\ \epsilon_y = {}^3/_2\,\bar{\epsilon}\ (3.15),\ \epsilon_z = {}^3/_2\,\bar{\epsilon}\ (3.97), \qquad [5]$$

and the directions of maximum and minimum absorption in the xz plane lie within 1.5° of the x and z axes. The absorption

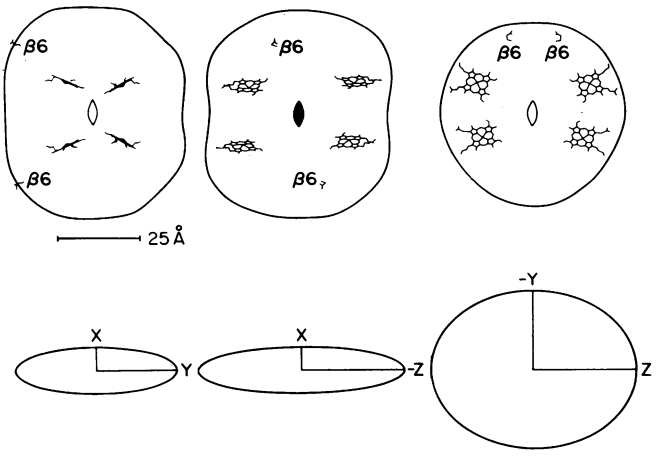

FIG. 2. Projection of molecular surface (*top*) and optical absorption ellipsoid (*bottom*) of the deoxyhemoglobin molecule. The views are down the true 2-fold molecular axis, y, and the pseudo-2-fold axes, x and z. The rough outline of the projected molecule is drawn from computer plots of a stick model using the 2.8-Å atomic coordinates of horse deoxyhemoglobin, whose structure is very similar to that of human deoxyhemoglobin A (16). The iron-porphyrins and β6 glutamic-acid residues are also shown. In deoxyhemoglobin S these two residues are replaced by valines.

ellipsoid is shown in Fig. 2 and predicts a maximum polarization ratio of $P = 4.05$ for a single uniaxial fiber.

To ascertain the accuracy of the calculated ellipsoid, we measured polarized absorption spectra of single crystals of deoxyhemoglobin A. The measurements were performed on the (010) face of this monoclinic crystal. Monoclinic symmetry requires that one principal absorption direction be parallel to the b crystal axis at all wavelengths; the other two orthogonal directions may lie anywhere in the ac (010) plane and may change with wavelength (22). This crystal, therefore, provides us with the opportunity to calculate not only the polarization ratio, but also the principal absorption directions from the x-ray structure. Our calculated absorption ellipsoid predicts that these directions are $-1.9°$ from the a and c^* crystal axes. We have observed that the directions of maximum and minimum absorption and the extinction directions occur at $-0.5 \pm 1°$ throughout the Soret band, in agreement with the calculated values. The predicted polarization ratio ($\epsilon_{c^*}/\epsilon_a$) is calculated from Eq. **5** by transforming the ellipsoid from the x,y,z molecular system into the a,b,c^* crystal system and is found to be 4.2. In Fig. 3 we show the absorption and polarization ratio spectrum in the Soret region of the (010) face of the deoxyhemoglobin A crystal. The polarization ratio varies through the band, reaching maximum and minimum values of 4.5 and 3.5, respectively. The fluctuation arises mainly from small splittings of the components of the degenerate Soret transition (17, 19, 20). At 430 nm, the peak of the solution absorption spectrum, the polarization ratio is 4.15, while the ratio of the areas under the c^* and a-polarized bands, integrated from 400 to 440 nm, is 3.9. We take the average of these two values, 4.0 ± 0.2, as our best estimate of the experimentally determined Soret polarization ratio, in essentially perfect agreement with the value predicted from the x-ray structure.

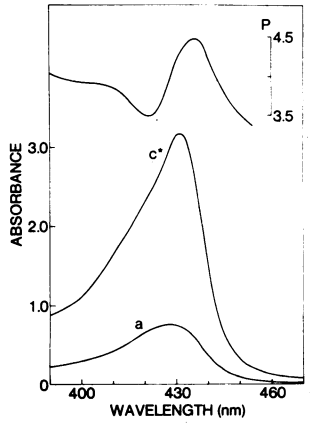

FIG. 3. Polarized absorption and polarization ratio spectrum of deoxyhemoglobin A single crystal on the (010) crystal face. The *upper* absorption spectrum is for incident light polarized parallel to the c^* crystal axis; the *lower* spectrum for light polarized parallel to the a crystal axis. The polarization ratio at each wavelength is plotted at the top of the figure and is defined as the ratio of the absorbances of c^* and a.

The remaining experimental problem is the determination of the polarization ratio, P, for a single fiber. Electron microscopy has revealed that optically resolvable regions exhibiting nearly perfect parallel orientation of individual fibers exist within sickled cells (8, 10, 13). Polarized absorption measurements on such regions should thus provide a good estimate of P. Upon microscopic examination of sickled cells, however, one finds an extremely wide variety of morphologies and a corresponding heterogeneity in their anisotropic optical properties. Not only does the magnitude of the birefringence differ markedly from cell to cell, but the extinction directions and birefringence may depend on the position within the cell. We attribute such positional variation to the presence of multiple domains of aligned fibers, and discriminate against such optically resolvable or "macroscopic" disorder by selecting regions of cells for photometric measurements that show uniform extinction. We also select cells in which the measuring region shows a well-defined long axis. In this way we can relate directions in cells to the fiber axes, since electron micrographs (8, 10, 13) also indicate that the long axis of a sickled cell is the preferred direction for the orientation of the long axis of the fibers. Observations on several hundred cells corroborate the electron micrographs by showing that whenever a long axis can be defined it corresponds to an extinction

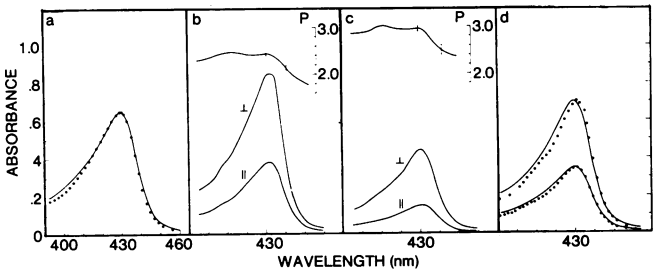

FIG. 4. Absorption spectra on about 1-μm^2 regions of deoxygenated human erythrocytes. (*a*) Normal erythrocytes: (*filled circles*) experimental points measured on a single cell; (*solid curve*) spectrum of a 1 mM solution of deoxyhemoglobin A. The solution spectrum is normalized to have the same maximum absorbance as the cell. (*b* and *c*) Sickled erythrocytes: (*lower spectrum*) light polarized parallel to the long axis of the cell; (*upper spectrum*) light polarized perpendicular to the long axis. (*d*) Isotropic spectra of deoxyhemoglobin S: (*filled circles*) isotropic absorption spectrum calculated from the polarized spectra in (*b*); (*open circles*) isotropic spectrum calculated from (*c*); (*solid curves*) spectra of a 1 mM deoxyhemoglobin S solution which have been normalized to have the same maximum absorbance as the calculated isotropic-cell spectra.

axis. A third criterion, necessary for accurate absorption measurements, is that the region of the cell to be measured have a uniform absorbance.

Fig. 4 shows absorption spectra through the Soret band on about 1-μm^2 regions of deoxygenated single cells. It is only the extremely high intensity of the Soret band [$\bar{\epsilon}_{max}$ = 133,000 M^{-1} cm^{-1} (28)] and the unusually high chromophore concentration ($\approx$0.02 M) which permit accurate absorption measurements on samples as thin as single erythrocytes (1–3 μm). The spectrum of a normal cell in Fig. 4*a* is in excellent agreement with the solution spectrum of deoxyhemoglobin A, providing an important test of the reliability of our measurements on these small sample areas. The polarization ratio observed for normal cells is 1.00 $\pm$ 0.03, indicating no net orientation of hemoglobin molecules in normal cells, as expected. Polarized absorption spectra on sickled cells are shown in Fig. 4*b* and *c*, together with the spectrum of the polarization ratios. To further test the reliability of the polarized spectra, we compared the isotropic absorption spectra calculated from the relation for a uniaxial system, $\overline{OD} = {}^1/_3 (OD_{||} + 2OD_{\perp})$, with those measured on a solution of deoxyhemoglobin S. Here again the agreement is quite good, although the slight red shift (<1 nm) of the calculated spectra may be outside our experimental error.

The spectra of the two sickled cells in Fig. 4 yield substantially different average polarization ratios. We have observed a continuum of highly reproducible values for the polarization ratio from 1 to 3; the spectrum of the polarization ratio shows the same basic features in all cells, suggesting that there is only a single detailed structure for the fibers.† Electron microscopy, together with our optical observations of regions of single cells having different extinction axes, leads to the hypothesis that the continuum of observed polarization ratios arises principally from the variability in the degree of alignment of fibers.‡ Our problem, then, is to determine the polarization ratio on a region of a cell free from this "microscopic" disorder. The approach we have taken is dictated by the distribution of the polarization ratios (Fig. 5). We see that the probability of finding cells with perfectly aligned fibers is low, suggesting two possible methods for obtaining the limiting value of P. First, we could collect data on a large enough sample of cells to accurately characterize the high orientation tail of the distribution. A rigorous application of this approach would require measurements on at least 1000 cells. A more expedient method, and the one we have used, is to search for cells with high polarization ratios and accept the highest measured value as a lower limit for the true value of P. Thus, extensive photometric measurements only need be performed on a limited number of cells. We have examined preparations of sickled cells from 10 different patients and the highest polarization ratio we have measured is 3.0 $\pm$ 0.1.§

† The fluctuation in the polarization ratio through the Soret band arises from a splitting of the degenerate components of this $\pi \rightarrow \pi^*$ transition (17, 19, 20). This splitting results from interactions between the porphyrin and its environment. We expect, therefore, that the polarization ratio spectrum will be sensitive to differences in both the structure of the hemoglobin molecule and its packing in the fiber.

‡ The presence of ungelled hemoglobin, e.g., hemoglobin F (14), in the measuring region, as well as experimental errors such as some tilting of the long axis of the cell out of the plane perpendicular to the light beam, should make only a minor contribution to the variability in the observed polarization ratio.

§ Convergence effects will produce a measured polarization ratio that is lower than the true value. We have chosen not to make any theoretical corrections to the measured values since our optical system is not ideal.

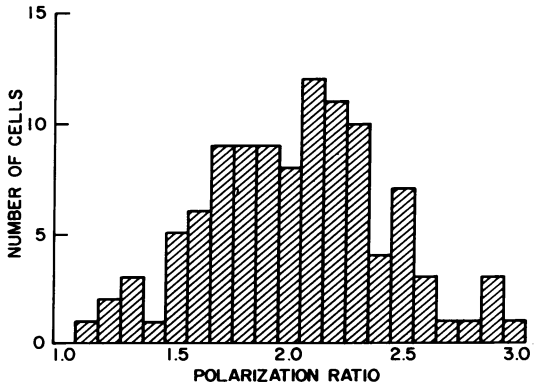

FIG. 5. The distribution of polarization ratios in sickled cells. Regions of sickled cells were selected by the criteria that they exhibit a well-defined long axis, uniform extinction, and uniform absorbance.

From our earlier results on the absorption ellipsoid of the hemoglobin molecule (Eq. **5**) and P = 3.0 $\pm$ 0.1, the maximum and minimum angles that the x molecular axis can make with the fiber axis are (Eq. **4**.): $\phi_x^{max} = 20°(+2°, -4°)$ and $\phi_x^{min} = 17°$ (+3°, −5°). The uncertainties in the ϕs include the maximum uncertainty in both P and the calculated ϵ_x, ϵ_y, and ϵ_z. Because 3.0 is a lower limit for P, these values become upper limits for the angles ϕ_x^{max} and ϕ_x^{min}.

DISCUSSION

One way of preventing and treating sickle-cell disease might be through the administration of stereospecific agents that reduce the tendency of hemoglobin S molecules to aggregate. To rationally explore this possibly the detailed structure of the sickle cell fiber, particularly the regions of intermolecular contact, must first be established. With the present information the only approach to this structural problem is to build models of the fiber by assembling molecules with the known conformation of deoxyhemoglobin A. The basic parameters of such a model structure are the position and orientation of the individual molecules. Our optical data require that the angle between the x axis of the hemoglobin molecule and the fiber axis be less than 22°. This result is independent of the specification of the molecular positions and is of immediate use as a test of present models for the structure of the fiber. Thus, the molecular orientation proposed by Murayama (11) can be ruled out, while the orientation proposed by both Finch *et al.* (8) and Edelstein *et al.* (29) are permitted.

By eliminating 93% of the possible allowed space for the orientation of the x axis, our optical data reduce the determination of the molecular orientation to a nearly one-dimensional search (i.e., a rotation about the x axis). In order to discuss possible intermolecular contacts, we must first specify the molecular positions. Of the three published models for the molecular positions (8, 11, 29) we have adopted that of Finch *et al.* (8) since it is most consistent with the electron-microscope and x-ray diffraction data. Finch *et al.* (8) further suggest an approximate model for the molecular orientation in which the true 2-fold axis (y) is radial and the x axis is parallel or nearly parallel to the fiber axis. This model, while compatible with our optical result, is unattractive because it suggests no specific role for the β6 mutation sites in the formation of the fiber. The β6 residues lie on the surface of the molecule, only a few angstroms from the xy plane (Fig. 2). The proposed

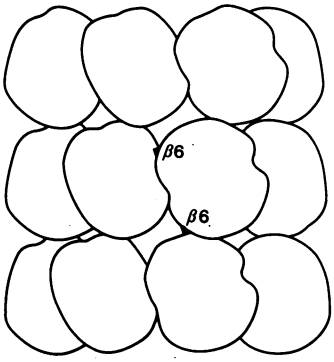

FIG. 6. A diagram of one of the three classes of models for the molecular orientation in the sickle-cell fiber which are permitted by the optical results and by the additional constraint that at least one β6 residue of each molecule be part of an intermolecular contact. The three central rings of Fig. 1 are depicted using rough molecular outlines taken from computer plots of stick model projections of horse deoxyhemoglobin. Both the maximum tilt of the x molecular axis allowed by the optical results and the cooperating helical rotation (7.3°) of the adjacent ring are necessary for the generation of an *inter*ring contact involving a β6 residue. This molecular orientation places the other β6 residue in position to make an *intra*ring contact.

orientation does not, therefore, permit β6 sites to be part of a contact between molecules in the fiber; they either point outward to the solvent or inward to the hollow core. Several considerations indicate that at least one β6 residue is part of, or very close to, an intermolecular contact within the fiber. Examination of the molecular structure of deoxyhemoglobin suggests that replacement of the glutamate at β6 with a valine should have only a local structural effect and should not significantly alter the overall tertiary or quaternary molecular conformation (8). Furthermore, it does not appear that the mutation site could be involved in a specific contact between fibers, since interfiber spacing in cells and gels can range from 180 to 240 Å (8). Also, sickling mutants (S, C_{Harlem}, $C_{Georgetown}$) all exhibit a mutation at or near the β6 site, while in various other surface mutants there has been no report of sickling (11, 30).

If we take as an additional constraint on the molecular orientation the requirement that at least one β6 site be part of an intermolecular contact, three classes of models are possible: (I) one β6 site is part of an *intra*ring contact (between adjacent molecules in the same ring) and the other β6 makes no contact; (II) both β6 sites are in (nonequivalent) *intra*ring contacts; and (III) one β6 site is part of an *intra*ring contact and the other is involved in an *inter*ring contact (between molecules in adjacent rings). In all three classes not only is there a small angle between the x molecular axis and the fiber axis, but the y axis also passes through some part of an adjacent molecule in the same ring. It is important to point out that in order to form an *inter*ring contact (class III) the maximum tilt of the x axis allowed by the optical data must be used (Fig. 6). The formation of an *inter*ring contact places the other β6 residue in position to make an *intra*ring contact. Thus, in all three classes of models a β6 residue could play a direct role in stabilizing *intra*ring contacts. Should more extensive polarized absorption measurements show that the angle between the x axis and the fiber axis is less than about 15°, the possibility of *inter*ring contacts (class III) involving β6 residues can be ruled out. We might conceivably find a decrease in the tilt of the x axis to this extent from additional measurements on cells or on gels, where preliminary measurements give maximum polarization ratios of about 2.5. The role of the β6 mutation would then be to stabilize *only intra*ring contacts. This role is consistent with the electron-microscope observation of irregularly aggregated filaments in deoxygenated normal cells (8).

We thank Dr. Pongrac Jilly, his staff, and patients at Freedmen's Hospital in Washington, D.C. for supporting this work with a continuous supply of sickle cell blood. We also thank Mr. Richard J. Feldmann for help in using his molecular modeling system, Drs. Andrew D. McLachlan and Max F. Perutz for providing us with hemoglobin atomic coordinates, Drs. Eduardo A. Padlan, Allen P. Minton, Beatrice Magdoff-Fairchild, and Elliot Charney for helpful and stimulating discussion, and Dr. John T. Finch for the preprint of his sickle-cell study.

1. Sherman, I. J. (1940) *Bull. Johns Hopkins Hosp.* **67**, 309–324.
2. Pauling, L., Itano, H. A., Singer, S. J. & Wells, I. C. (1949) *Science* **110**, 543–548.
3. Perutz, M. F. & Mitchison, J. M. (1950) *Nature* **166**, 677–679.
4. Harris, J. W. (1950) *Proc. Soc. Exp. Biol. Med.* **75**, 197–201.
5. Allison, A. C. (1957) *Biochem. J.* **65**, 212–219.
6. Bessis, M., Nomarski, G., Thiery, J. P. & Breton-Gorius, J. (1958) *Rev. Hematol.* **13**, 249–270.
7. Murayama, M., Olson, R. A. & Jennings, W. H. (1965) *Biochim. Biophys. Acta* **94**, 194–199.
8. Finch, J. T., Perutz, M. F., Bertles, J. F. & Dobler, J. (1973) *Proc. Nat. Acad. Sci. USA* **70**, 718–722.
9. Magdoff-Fairchild, B., Swerdlow, P. H. & Bertles, J. F. (1972) *Nature* **229**, 217–219.
10. Stetson, C. A. (1966) *J. Exp. Med.* **123**, 341–346.
11. Murayama, M. (1966) *Science* **153**, 145–149.
12. White, J. G. (1968) *Blood* **31**, 561–579.
13. Dobler, J. & Bertles, J. F. (1968) *J. Exp. Med.* **127**, 711–716.
14. Bertles, J. F., Rabinowitz, R. & Dobler, J. (1970) *Science* **169**, 375–377.
15. Muirhead, H., Cox, J. M., Mazzarella, L. & Perutz, M. F. (1967) *J. Mol. Biol.* **28**, 117–156.
16. Bolton, W. & Perutz, M. F. (1970) *Nature* **228**, 551–552.
17. Eaton, W. A. & Hochstrasser, R. M. (1967) *J. Chem. Phys.* **46**, 2533–2539.
18. Dickerson, R. E., Takano, T., Eisenberg, D., Kallai, O. B. Samson, L., Cooper, A. & Margoliash, E. (1971) *J. Biol. Chem.* **246**, 1511–1535.
19. Eaton, W. A. & Hochstrasser, R. M. (1968) *J. Chem. Phys.* **49**, 985–995.
20. Makinen, M. W. & Eaton, W. A. (1973) *Ann. N.Y. Acad. Sci.* **206**, 210–222.
21. Craig, S. P. & Walmsley, S. H. (1968) *Excitons in Molecular Crystals* (W. A. Benjamin, Inc., New York).
22. Born, M. & Wolf, E. (1959) *Principles of Optics* (Pergamon Press, London).
23. Eaton, W. A. & Lewis, T. P. (1970) *J. Chem. Phys.* **53**, 2164–2172.
24. Perutz, M. F. (1968) *J. Cryst. Growth* **2**, 54–56.
25. Muirhead, H. & Perutz, M. F. (1963) *Nature* **199**, 633–639.
26. Perutz, M. F., Trotter, I. F., Howells, E. R. & Green, D. W. (1955) *Acta Crystallogr.* **8**, 241–245.
27. Morell, S. A., Ayers, V. E. & Patkar, S. (1970) *Physiol. Chem. Phys.* **2**, 467–476.
28. Antonini, E. & Brunori, M. (1971) *Hemoglobin and Myoglobin in Their Reactions with Ligands* (North Holland, Amsterdam).
29. Edelstein, S. J., Telford, J. N. & Crepeau, R. H. (1973) *Proc. Nat. Acad. Sci. USA* **70**, 1104–1107.
30. Perutz, M. F. & Lehmann, H. (1968) *Nature* **219**, 902–909.